第32卷第12期　　焊　接　学　报　　Vol. 32　No. 12
2011年12月　TRANSACTIONS OF THE CHINA WELDING INSTITUTION　December　2011

激光对脉冲 MAG 电弧辐射的影响

刘德深[1]，李　桓[1]，王旭友[2]，王　威[2]，高　莹[3]
(1. 天津大学 天津市现代连接技术重点实验室，天津　300072; 2. 哈尔滨焊接研究所，哈尔滨　150080;
3. 天津职业技术师范大学 天津市高速切削与精密加工重点实验室，天津　300222)

摘　要: 搭建了激光-脉冲 MAG 复合焊接系统和采集系统，分别在加激光和不加激光的条件下进行试验，得到了电信号和电弧光谱数据. 运用线性拟合的方法，分析了 FeII274.648，FeI382.043，FeI492.050，ArI801.479 谱线的电弧能量输入和光谱辐射强度之间的关系. 结果表明，四条特征谱线的光谱辐射与电弧的能量输入成正比例的关系. 在相同的电弧能量输入下，激光-脉冲 MAG 复合焊的电弧辐射强度比脉冲 MAG 焊的电弧辐射强度小. 这是由于激光束产生的金属蒸气与光致等离子体对电弧等离子体辐射的吸收造成的.

关键词: 激光复合焊; 能量输入; 辐射强度; 线性拟合
中图分类号: TG403　　文献标识码: A　　文章编号: 0253-360X(2011)12-0021-04


刘德深

0　序　　言

激光和电弧复合热源焊接技术由英国学者 Steen 于 20 世纪 70 年代末期首次提出，其主要思想就是有效利用电弧能量，在较小的激光功率条件下获得较大的焊缝熔深，同时提高激光焊接对焊缝间隙的适应性，实现高效率、高质量的焊接过程[1-3]. 要实现激光复合焊的广泛使用，必须要对复合焊接的机理进行研究. Abe，kutsuna 等人[4,5]采用高速摄像观测了不同熔滴过渡形式下复合热源焊接过程中激光与电弧等离子体对熔池稳定性的影响. 大连理工大学的郝心锋和宋刚等人[6]通过建立激光-TIG 复合焊接和光谱采集系统，通过光谱辐射来分析激光与电弧的相互作用. 文中结合激光-脉冲 MAG 复合焊接系统以及电信号和光谱采集系统，比较激光复合与未复合条件下焊接电弧能量输入与电弧光谱辐射强度之间的关系，研究激光对脉冲 MAG 电弧辐射强度的影响.

1　试验原理

为了研究激光对脉冲 MAG 电弧辐射的影响，文中搭建了激光-脉冲 MAG 复合焊接系统和采集系统. 采集系统由电流、电压传感器、光谱仪和计算机构成. 为了使电信号和光谱信号有严格的对应关系，采集系统必须能够对这些信号进行同步采集.

由于影响电弧光谱辐射变化的因素很多，为了保证试验数据的可靠性，在其它焊接参数和条件不变的情况下，试验分别在激光复合与未复合的条件下进行，最终得到了不同脉冲对应下的电信号和电弧光谱辐射强度的数据. 为了综合焊接电流和电压的作用，采用了电弧能量输入作为一个变量. 在激光复合与未复合条件下，某一脉冲对应着特定的电弧能量输入和电弧光谱辐射强度. 运用数据拟合的办法，可以更直观地体现两种焊接条件下电弧能量输入对应电弧光谱辐射强度关系的区别，从而研究激光对电弧辐射所产生的影响.

2　试验设备及结果分析

2.1　试验系统构成

试验采用奥地利 Fronius 公司生产的 TPS 5000 型数字化焊接电源. 所用激光器为德国 HASS 公司生产的最大额定功率为 2 kW 的 HL2006D 型 Nd:YAG 激光器. 熔滴过渡方式为一脉一滴，使用 82% Ar + 18% CO_2 混合气体作为保护气体. 工件为 Q235 普通钢板，焊接方式为平板堆焊. 试验的焊接工艺参数如表 1 所示.

试验使用的光谱仪采用荷兰 Avantes 公司的

收稿日期: 2010-10-29
基金项目: 国家自然科学基金项目(51175374)；国家"十一五"科技支撑计划资助项目(2006BAF04B10)；天津市应用基础及前沿技术研究计划项目(09JCYBJC05000)；天津市科技支撑计划重点项目(10ZCKFSF00200)

表1 激光-脉冲 MAG 复合焊接试验参数

Table 1 Welding parameters in laser-MAG hybrid welding

电弧电压 U/V	焊接电流 I/A	焊接速度 v_w/(m·min^{-1})	气体流量 q/(L·min^{-1})	激光功率 P/W
21	150	0.15	17	2 000

Avaspec-2048 光纤式数字光谱仪,可以对 200 ~ 1 100 nm 波段范围的光谱进行采集. 计算机安装有研华数据采集卡 PCI-1716,负责触发信号及采集数据. 试验中焊接电信号的采样频率为 62.5 kHz,光谱仪由于自身性能和同步采集要求的限制,采样频率为 4 Hz,采样持续时间为 2 ms. 2 ms 的采样持续时间相对于整个焊接过程可认为是瞬时值.

在试验中,复合焊接机头固定不动,由行走小车承载焊接工件运动完成焊接试验. 光谱仪的光纤探头固定在焊接工作台上,作用在垂直焊接方向靠近电弧位置的一侧,以获得电弧的光谱信息. 试验分别在加激光和不加激光的条件下进行. 采集系统与复合焊接系统的连接如图 1 所示.

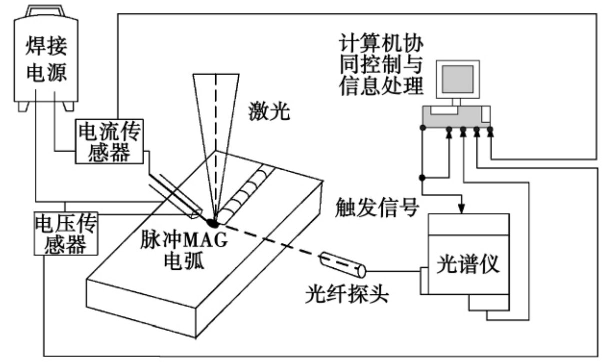

图1 焊接系统及采集系统连接示意图

Fig. 1 Schematic of welding and data acquisition system

2.2 激光复合前后电弧光谱的分布情况

在每个触发脉冲下电弧的能量输入 E 是电功率在 2 ms 内的积分,其表达式为

$$E = \int_{t_0}^{t_f} ui\mathrm{d}t \tag{1}$$

式中: u 为采样得到的瞬时电压; i 为采样得到的瞬时电流; t_o 为触发脉冲对应的开始时间; t_f 为 2 ms 采样结束的时间. 图 2 为不同焊接条件下光谱在 200 ~ 1 000 nm 分布. 通过图 2 可以看出,激光加入后电弧能量 E 为 18.546 1 J 时的光谱辐射强度并不比脉冲 MAG 焊中电弧能量 E 为 17.364 7 J 时的辐射强度大,反而有所减弱. 由此可见,在电弧能量输入基本相同的情况下,激光复合前后电弧光谱辐射强度是有区别的.

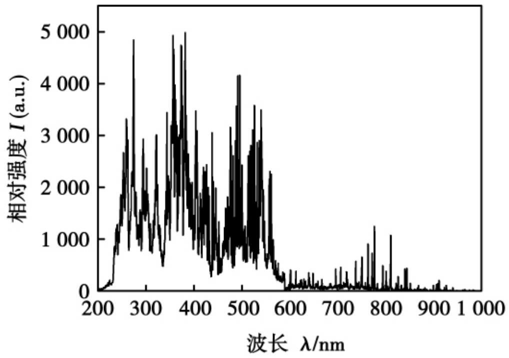

(a) 激光未复合 E=17.3647 J

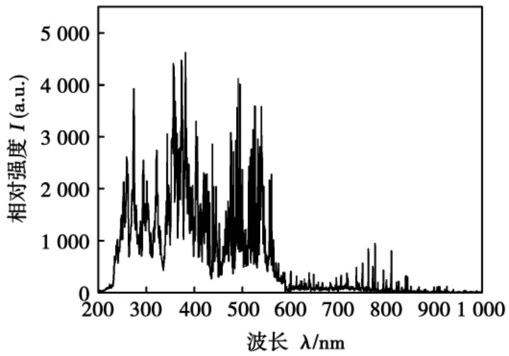

(b) 激光复合 E=18.5461 J

图2 不同焊接条件下光谱在 200 ~1 000 nm 的分布

Fig. 2 Spectral distribution of different welding condition in 200 - 1 000 nm

2.3 激光复合前后能量输入与光谱辐射的关系

电弧等离子体的光谱辐射主要由 250 ~ 340 nm 的 FeI,FeII 谱线辐射,340 ~ 600 nm 的 FeI 谱线辐射和 600 ~ 900 nm 的 ArI 谱线辐射构成. 为了剔除其它谱线的干扰,在这些区域中取出具有代表性的特征谱线进行研究,分别为 FeII274.648,FeI382.043,FeI492.050,ArI801.479.

运用最小二乘法,分别对这四条特征谱线的辐射强度随能量输入的变化规律进行线性拟合,得到了激光复合与未复合条件下各个脉冲的能量输入和辐射强度的对应关系结果,如图 3 所示. 其中,x 为自变量,是每个触发脉冲下电弧的能量输入; y 为变量是能量输入对应下的光谱辐射强度.

一元线性拟合的基本形式为 $y = ax + b$,其中 a 为直线关系式的斜率,b 为关系式的常数项. 对于文中试验拟合的结果,常数项代表了拟合结果和理想情况的偏差. 由图 3 可以知道,无论是脉冲 MAG 焊接还是激光-脉冲 MAG 复合焊接,FeII274.648,FeI382.043,FeI492.050 和 ArI801.479 谱线的辐射强度都随着电弧能量输入的增加而增加. 也就是说,光谱辐射与电弧的能量输入成正比例的关系,这个比例就是拟合直线的斜率. 其中,图3a直线斜率

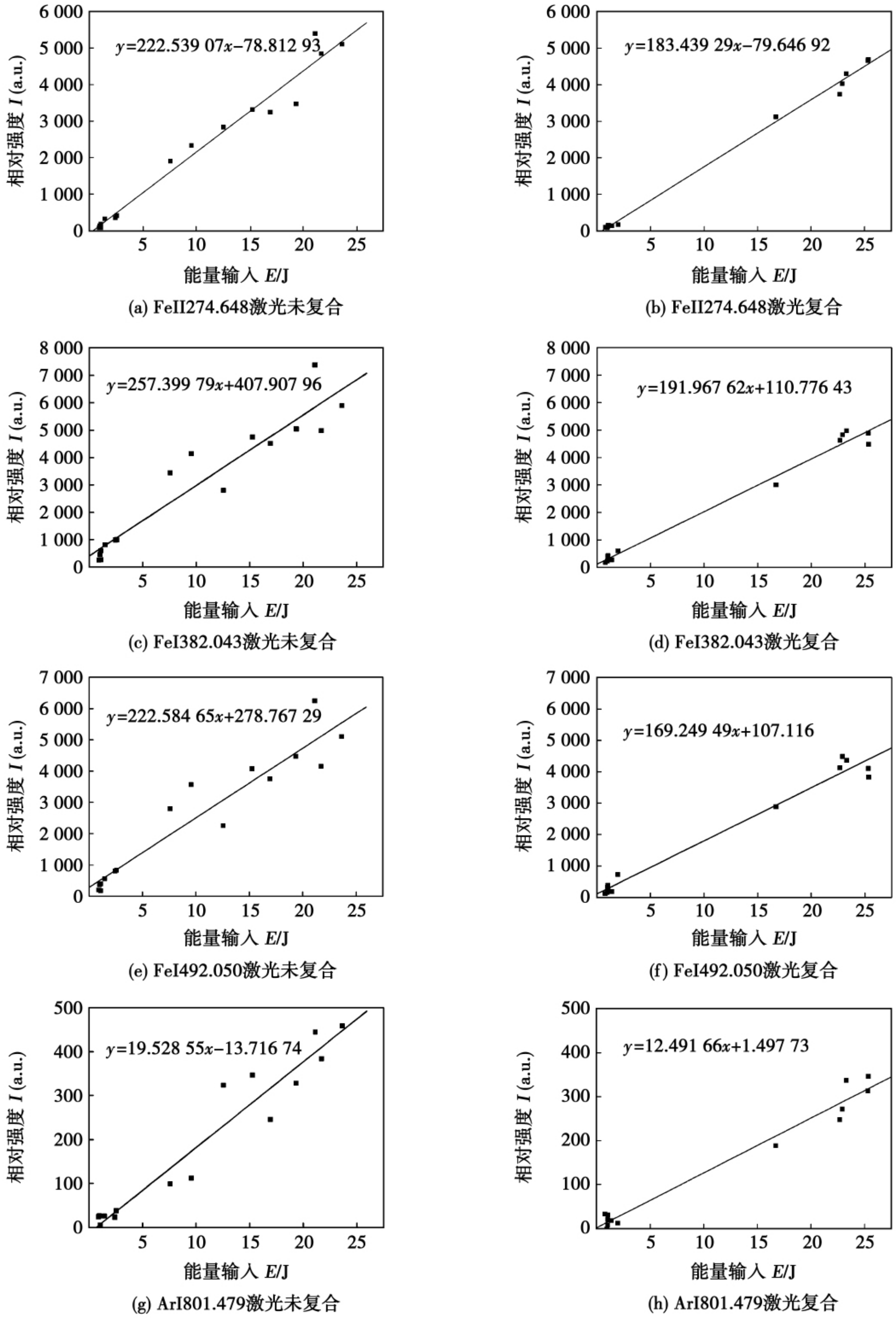

(a) FeII274.648激光未复合　(b) FeII274.648激光复合

(c) FeI382.043激光未复合　(d) FeI382.043激光复合

(e) FeI492.050激光未复合　(f) FeI492.050激光复合

(g) ArI801.479激光未复合　(h) ArI801.479激光复合

图 3　激光复合前后的能量输入和辐射强度的对应关系

Fig. 3　Relation between energy input and intensity of MAG welding and hybrid welding

为 222.539 07；图 3b 直线斜率为183.439 29；图 3c 直线斜率为 257.399 79；图 3d 直线斜率为191.967 62；图 3e 直线斜率为 222.584 65；图 3f 直线斜率为 169.249 49；图 3g 直线斜率为 19.528 55；图 3h 直线斜率为 12.491 66.

通过比较激光复合前后的拟合结果可以发现，在文中试验条件下，四条谱线的激光复合焊拟合直线的斜率都要比单纯脉冲 MAG 焊拟合直线的斜率有不同程度的减小，即在相同的电弧能量输入下，激光-脉冲 MAG 复合焊的电弧辐射强度比脉冲 MAG 焊的电弧辐射强度小. 通过计算，比较图 3a 和图 3b，图 3c 和图 3d，图 3e 和图 3f，图 3g 和图 3h，发现

激光加入后,FeII274.648 谱线斜率下降了 17.6%, FeI382.043 谱线斜率下降了 25.4%,FeI492.050 谱线斜率下降了 24.0%,ArI801.479 谱线斜率下降了 36.0%. 降幅比例越大,则反映出激光对该谱线的辐射强度影响越大. 由此可见,激光对 FeI382.043, FeI492.050 和 ArI801.479 谱线辐射强度的影响比较大,其中对 ArI801.479 谱线辐射强度的影响是最大的.

激光-脉冲 MAG 复合焊时,激光和电弧之间存在较强的相互作用. 激光的能量密度大,使金属材料在短时间内蒸发,产生大量的金属蒸气以及少量的光致等离子体. 根据文中所得到的试验结果可以看出,激光束产生的金属蒸气与光致等离子体对电弧等离子体辐射具有吸收作用. 激光与电弧的相互作用实际上是激光与等离子体的相互作用. 逆韧致辐射吸收是等离子体吸收的主要机制. 逆韧致辐射吸收后电弧能量的减弱遵循下面的衰减规律,即

$$I_1 = I_0 e^{-\alpha \Delta y} \tag{2}$$

式中: I_0 为电弧等离子初始的能量密度; Δy 为电弧通过激光等离子体内部的距离; I_1 是经过 Δy 距离后电弧的能量密度; α 是等离子体的吸收系数. 计算激光致等离子逆韧致辐射吸收系数有一个简易计算公式,即

$$\alpha = kN^2/\sqrt{T} \tag{3}$$

式中: k 是一个跟激光波长有关的系数; N 是粒子的密度; T 为金属蒸气的温度. 可见粒子密度越大,吸收系数越大. 所以高能量密度激光对金属加热产生的大量粒子通过逆韧致辐射吸收削弱了电弧等离子体辐射[7]. 因为激光对 ArI801.479 谱线辐射强度的影响最大,所以激光致等离子体对 Ar 粒子辐射的吸收更为强烈,这也体现出在氩气氛时激光对电弧的影响强烈[8]. 另外,激光对部分电弧等离子体辐射的吸收减小了电弧中等离子体对激光的阻碍作用,使激光能量的传输得到增强,因此这种吸收作用对激光电弧复合焊焊接效率的提升也具有积极作用.

3 结 论

(1) 搭建了激光-脉冲 MAG 复合焊接系统和采集系统,试验分别在加激光和不加激光的条件下进行. 得到了电信号和电弧光谱数据.

(2) 无论是脉冲 MAG 焊接还是激光-脉冲 MAG 复合焊接,FeII274.648,FeI382.043,FeI492.050 和 ArI801.479 这四条特征谱线的辐射强度都随着电弧能量输入的增加而增加,并且成一定的比例关系.

(3) 通过激光复合前后的比较可以发现, FeII274.648,FeI382.043,FeI492.050 和 ArI801.479 谱线的激光复合拟合直线的斜率都要比未复合拟合直线的斜率有不同程度的减小,在相同的电弧能量输入下,激光-脉冲 MAG 复合焊的电弧辐射强度比脉冲 MAG 焊的电弧辐射强度小.

(4) 激光-脉冲 MAG 复合焊时,激光和电弧之间存在较强的相互作用. 根据文中所得到的试验结果可以看出,激光束产生的金属蒸气与光致等离子体对电弧等离子体辐射具有吸收作用,这种吸收作用对激光电弧复合焊焊接效率的提升也具有积极作用.

参考文献:

[1] Eboo M, Steen W M, Clark J, Arc augmented laser processing of materials, Advances in welding process [C] // 4th Interational Conference, Harrogate, UK, 1978: 257-265.

[2] Steen W M, Eboo M. Arc augmented laser welding [J]. Metal Construction, 1979, 11(7): 332-335.

[3] Steen W M. Arc augmented laser processing of material [J]. Journal of Applied Physics, 1980, 51(11): 5636-5641.

[4] Abe N, Kunugita Y, Hayashi M, *et al*. Dynamic observation of high speed laser-arc combination welding of thick steel plates [J]. Transactions of JWRI, 1997, 26(2): 7-11.

[5] Kutsuna M, Chen L. Interaction of both plasmas in CO_2 laser-MAG hybrid welding of carbon steel [C] // First International Symposium on High-power Laser Macro-processing, Osaka, Japan, 2002: 314-346.

[6] Hao Xinfeng, Song Gang. Spectral analysis of the plasma in low-power laser/arc hybrid welding of magnesium alloy [J]. IEEE Transactions on Plasma Science, 2009, 37(1): 76-82.

[7] Miller R, DebRoy T. Energy absorption by metal-vapor-dominated plasma during carbon dioxide laser welding of steels [J]. Journal of Applied Physics, 1990, 68(5): 2046-2050.

[8] 吴世凯, 肖荣诗, 张寰臻. 电弧气氛对 CO_2 激光与 TIG 电弧相互作用的影响 [J]. 焊接学报, 2009, 30(10): 81-85.
Wu Shikai, Xiao Rongshi, Zhang Huanzhen. Effect of arc atmosphere on interaction of CO_2 laser beam and TIG arc [J]. Transactions of the China Welding Institution, 2009, 30(10): 81-85.

作者简介: 刘德深,男,1986 年出生,硕士. 主要从事激光复合焊和脉冲 TIG 焊的焊接工艺研究. Email: liudeshen@tju.edu.cn

通讯作者: 李 桓,男,教授. Email: lihuan@tju.edu.cn chine DU Suigeng, YANG Zhengqiang, YU Longqi (Key Laboratory of Ministry of Education for Contemporary Design and Integrated Manufacturing Technology, Northwestern Polytechnical University, Xi´an 710072, China). p 17 – 20

Abstract: In view of the issues that the control effect of the load system of friction welding machine on pressure mutation phases is unsatisfactory with (proportion integration) closed-loop control algorithm, the fuzzy PI control algorithm is introduced. According to the error and its changing trend of the actual value and the set value, the whole control process is divided into four kinds of control intervals. Based on optimizing the fuzzy control degree, the corresponding fuzzy rules and parameters determining methods are developed. Under the test conditions, the control effects of four control intervals with the different control parameters are contrasted, the best fit coefficients of every control interval are obtained. The performance indicators using fuzzy PI control methods are better than that using traditional PI control methods. Under test conditions with the optimizing fuzzy control degree and the best fit coefficients, the maximum overshoot has been reduced 19.2%, the adjust time has been reduced 1.59 s, and the steady precision has been raised 0.4%.

Key words: friction welding machine; computer control; fuzzy-PI; control algorithm

Effect of laser on pulsed MAG arc radiation LIU Deshen[1], LI Huan[1], WANG Xuyou[2], WANG Wei[2], GAO Ying[3] (1. Tianjin Key Laboratory of Advanced Joining Technology, Tianjin University, Tianjin 300072, China; 2. Harbin Welding Institute, Harbin 150080, China; 3. Tianjin Key Laboratory of High Speed Cutting and Precision Machining, Tianjin University of Technology and Education, Tianjin 300222, China). p 21 – 24

Abstract: The laser-pulsed MAG hybrid welding system and acquisition system were set up to get the electric signal and arc spectrum under the conditions with and without laser. To analyze the relationship between arc energy input and the spectral radiation intensity of FeII274.648, FeI382.043, FeI492.050 and ArI801.479 using the method of linear fit. Studies have shown that the spectral radiation intensity of the four feature spectrum lines are proportion to arc energy input. With the same arc energy input, the arc radiation intensity of hybrid welding is smaller than the one of pulsed MAG welding. This is because the metal vapor and plasma produced by laser may absorb the arc plasma radiation.

Key words: laser hybrid welding; energy input; radiation intensity; linear fit

Microstructure of solder joints with micron stand-off height in electronic packaging WANG Bo[1,2], MO Liping[1], WU Fengshun[1,2], XIA Weisheng[1], WU Yiping[1,2] (1. State Key Laboratory of Material Processing and Die & Mould Technology, Huazhong University of Science and Technology, Wuhan 430074, China; 2. Wuhan National Laboratory for Optoelectronics, Wuhan 430074, China). p 25 – 28

Abstract: In present paper the microstructural change was studied when the stand-off height (SOH) of solder joints with Cu/Sn/Cu sandwich structure was reduced from 100 μm to 50 μm, 20 μm and 10 μm. With the reducing stand-off height, the Cu content increases in the solder bulk, and the Cu_6Sn_5 intermetallic layer formed at both sides decreases in thickness; while the proportion of IMC thickness to solder joint stand-off height increases. The thickness of the copper layer consumed by solder joints with different stand-off heights was calculated according to the formed IMC layer and Cu content in the solder bulk. It is found that the consumed copper thickness decreases with the reducing stand-off height. In the aging, the solder joint with lower SOH increases faster in IMC thickness and IMC proportion, leading to more dramatic microstructural change.

Key words: electronic packaging solder joint; stand-off height; micro structure

Morphologies and growth mechanism of TiN in ceramic surface layers prepared by nitrogen arc ZHENG Xiaoyi[1], CONG Dazhi[2], LI Xin[1], ZHAO Lei[1], LI Yuhua[1], REN Zhenan[1] (1. College of Materials Science and Engineering, Jilin University, Changchun 130022, China; 2. Shanghai Nuclear Engineering Research & Design Institute, Shanghai 200233, China). p 29 – 32

Abstract: The titanium nitride (TiN) ceramic surface layers were in-situ prepared by nitrogen arc melting on the surface of pure titanium substrates. The formation mechanism of the ceramic layers, the growth morphologies and mechanism of the TiN phase were investigated. The results show that the nitrogen arc melting is a non-equilibrium rapid cooling process and the cooling rate can be as high as $10^2 \sim 10^3$ K/s. The micro growth modes of the TiN phase in ceramic surface layers exhibit the diversity. The TiN crystal grows up by the spiral dislocation lateral growth mode at the location of low undercooling in the molten pool. Because of the undercooling increased at the bottom of the molten pool, the micro growth mode changes to the alternating between the continuous growth and the lateral growth.

Key words: nitrogen arc; titanium nitride; morphology; growth mechanism

Bonding mechanism of brazing of amorphous Cu-P filler metal ZOU Jiasheng, WANG Chao, XU Xiangping, WANG Lei (Provincial Key Lab of Advanced Welding Technology, Jiangsu University of Science and Technology, Zhenjiang 212003, China). p 33 – 36

Abstract: The copper joints were brazed with CuP 7.7 Sn5.4Ni14Si0.2Zr0.04 amorphous filler metal conventional filler metal respectively. The effect of the brazing temperature and time on the crystalline composition and microstructure of joints brazed with the amorphous brazing filler metal were compared and analyzed by micro-method. The results showed that the joints brazed with CuP7.7Sn5.4Ni14Si0.2Zr0.04 amorphous brazing filler metal consist of centre zone, interface area and diffusion zone. With the increase of brazing temperature and brazing holding time, the interface area brazed with both amorphous and conventional filler metal increases, and the microstructures of base metal and brazinrg seam centre zone would be coarsed. Excessively high brazing temperature or long brazing holding time will produce brittle phase, but this effect on amorphous filler metals is much smaller. Under the same conditions, amorphous filler metals interact with the base metal much more intensely than the corresponding conventional filler metals. The microstructure in interface area and centre zone of amorphous brazing seam are evidently uniform and small.

Key words: Cu-P based filler metal; amorphous filler